The Resistive Bifurcated Parallel-Plate Waveguide

HAO-MING SHEN

Abstract—**The guided-wave problem of a parallel-plate region with a bifurcating resistive sheet of finite length is solved. After the space has been divided into three regions, the series solutions in them are matched across the boundaries. Then, the eigenequation is used to determine the propagation and four sets of equations are solved for the unknown coefficients. The series solutions converge rapidly and are readily applied to obtain conditions of maximum absorption.**

I. Introduction

OFTEN in a guided-wave system higher mode electromagnetic waves are excited by a nonuniform structure, and it is desired to absorb them without affecting the principal mode. One method is with resistive material in a specific location as shown in Fig. 1. Consider a TEM wave that propagates in an infinite parallel-plate region in the z-direction together with some of the lower TM and TE modes. In order to absorb only the TM and TE waves, a resistive sheet can be placed halfway between the parallel plates where both the TM and TE modes have parallel components, E_x and E_z, but the TEM mode does not. The purpose of this paper is to solve this boundary-value problem and get a theoretical representation of the TM and TE waves, from which we can determine the resistance R and width w of the resistive sheet which provide the maximum absorption.

Only a few complex boundary-value problems have been solved exactly and these have been accomplished by integral transform techniques and the method of separation of variables [1]. In many boundary-value problems one cannot find a coordinate system in which the coordinate surfaces coincide with the boundaries in the whole region. In this case, we can separate the space being considered into several regions. The new regions must be divided so that in each of them the coordinate surfaces can coincide with the new boundaries completely. Then we let the formal series solutions in the different regions match the boundary conditions; these include the interfaces between the new regions. This idea has been used to solve problems of radiation and scattering by a finite cone [2], [3], and problems of waveguide discontinuities [4]. Recently a scattering problem involving a more complex shape, such as a spherical mirror, has been solved using this approach [5]. In the present paper we apply this method to solve the problem of the resistive bifurcated parallel-plate waveguide.

Manuscript received June 26, 1980; revised July 24, 1980. This work was supported in part by the Joint Services Electronics Program under Contract N00014-75-C-0648 with Harvard University.

The author is with the Gordon McKay Laboratory, Harvard University, Cambridge, MA 02138.

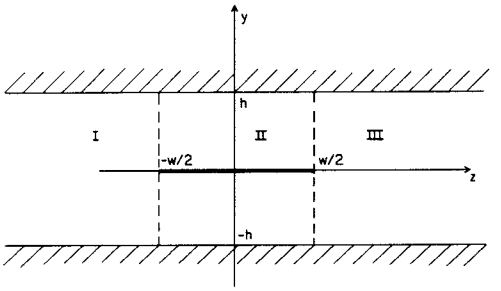

Fig. 1. The resistive bifurcated parallel-plate waveguide.

II. The Boundary Conditions

Suppose the parallel-plate region is infinite in both the x- and z-directions and the electromagnetic waves propagate in the z-direction. It follows that the fields are x-independent. The y- and z-components of the fields can be expressed in terms of E_x and H_x which satisfy the Helmholtz equation and represent TE and TM waves, respectively. They are

$$H_y = \frac{1}{j\omega\mu_0}\frac{\partial E_x}{\partial z}$$

$$H_z = -\frac{1}{j\omega\mu_0}\frac{\partial E_x}{\partial y}$$

$$E_y = -\frac{1}{j\omega\epsilon_0}\frac{\partial H_x}{\partial z}$$

$$E_z = \frac{1}{j\omega\epsilon_0}\frac{\partial H_x}{\partial y}. \tag{1}$$

The boundaries of the parallel-plate region are at $y = \pm h$, $z = \pm\infty$, and $y = \pm 0$, $|z| \leqslant w/2$. The boundary of the resistive sheet coincides with only part of the $y = 0$ surface. For this reason, we separate the space in the parallel-plate region into the three parts: $z \leqslant -w/2$, $-w/2 \leqslant z \leqslant w/2$, $w/2 \leqslant z$, which are denoted, respectively, by I, II, III. In each of these regions the new boundaries coincide completely with some coordinate surfaces. For instance, in region II the boundaries coincide with the coordinate surfaces: $y = \pm h$, $y = \pm 0$, $z = \pm w/2$. Let the fields $\bar{E}$ and $\bar{H}$ with subscripts I, II, III represent the fields in the three regions. The boundary conditions are: $E_x = E_z = 0$ for $y =$

0018-9480/80/1100-1192$00.75 ©1980 IEEE

$\pm h$; $\bar{E}_{\mathrm{I}}=\bar{E}_{\mathrm{II}}$, $\bar{H}_{\mathrm{I}}=\bar{H}_{\mathrm{II}}$ for $z=-w/2$, $|y|\leqslant h$; $\bar{E}_{\mathrm{II}}=\bar{E}_{\mathrm{III}}$, $\bar{H}_{\mathrm{II}}=\bar{H}_{\mathrm{III}}$ for $z=+w/2$, $|y|\leqslant h$. These imply that

$$\text{for } z=-w/2\text{: } E_{x\mathrm{I}}=E_{x\mathrm{II}} \qquad \frac{\partial E_{x\mathrm{I}}}{\partial z}=\frac{\partial E_{x\mathrm{II}}}{\partial z} \tag{2a}$$

$$H_{x\mathrm{I}}=H_{x\mathrm{II}} \qquad \frac{\partial H_{x\mathrm{I}}}{\partial z}=\frac{\partial H_{x\mathrm{II}}}{\partial z} \tag{2b}$$

$$\text{for } z=w/2\text{: } E_{x\mathrm{II}}=E_{x\mathrm{III}} \qquad \frac{\partial E_{x\mathrm{II}}}{\partial z}=\frac{\partial E_{x\mathrm{III}}}{\partial z} \tag{3a}$$

$$H_{x\mathrm{II}}=H_{x\mathrm{III}} \qquad \frac{\partial H_{x\mathrm{II}}}{\partial z}=\frac{\partial H_{x\mathrm{III}}}{\partial z}. \tag{3b}$$

When $y=0$, $|z|\leqslant w/2$, there are two cases.

Case 1: When $d\ll\delta$, $d\ll\lambda$, we have $E_{x\mathrm{II}}(0+,z)=E_{x\mathrm{II}}(0-,z)$; $E_{z\mathrm{II}}(0+,z)=E_{z\mathrm{II}}(0-,z)$; $H_{z\mathrm{II}}(0+,z)-H_{z\mathrm{II}}(0-,z)=E_{x\mathrm{II}}(0,z)/R$; $H_{x\mathrm{II}}(0+,z)-H_{x\mathrm{II}}(0-,z)=-E_{z\mathrm{II}}(0,z)/R$, where d is the thickness of the sheet, δ is the depth of the penetration, and R is the resistance of a square meter of the sheet. It follows that

$$E_{x\mathrm{II}}(0+,z)=E_{x\mathrm{II}}(0-,z) \tag{4}$$

$$\left.\frac{\partial H_{x\mathrm{II}}}{\partial y}\right|_{y=0+}=\left.\frac{\partial H_{x\mathrm{II}}}{\partial y}\right|_{y=0-} \tag{5}$$

$$\left.\frac{\partial E_{x\mathrm{II}}}{\partial y}\right|_{y=0+}-\left.\frac{\partial E_{x\mathrm{II}}}{\partial y}\right|_{y=0-}=-j\omega\mu_0 E_{x\mathrm{II}}(0,z)/R \tag{6}$$

$$H_{x\mathrm{II}}(0+,z)-H_{x\mathrm{II}}(0-,z)=j\left.\frac{\partial H_{x\mathrm{II}}}{\partial y}\right|_{y=0}\Big/R\omega\epsilon_0. \tag{7}$$

Case 2: When $\delta\ll d\ll\lambda$, we have $H_{z\mathrm{II}}(0+,z)=E_{x\mathrm{II}}(0+,z)/R^+$; $H_{x\mathrm{II}}(0+,z)=-E_{z\mathrm{II}}(0+,z)/R^+$; $-H_{z\mathrm{II}}(0-,z)=E_{x\mathrm{II}}(0-,z)/R^-$; $H_{x\mathrm{II}}(0-,z)=E_{z\mathrm{II}}(0-,z)/R^-$, where R^+ or R^- is the upper or lower skin resistance. From the geometrical symmetry of the incident field it follows that $E_{x\mathrm{II}}(0+,z)=E_{x\mathrm{II}}(0-,z)$ and $E_{z\mathrm{II}}(0+,z)=\mathrm{E}_{z\mathrm{II}}(0-,z)$. These yield conditions of the same form as (4)–(7). However, $1/R=1/R^++1/R^-$ where R is still the resistance per unit area of the sheet.

III. General Solution

Consider the TM wave for which $E_x=0$. The general solutions for the different regions are:

Region I: Both incident and reflected fields exist in this region. The incident field can be expanded as follows:[1]

$$H_{xi}(y,z)=\sum_{n=0} g_n \sin\left(\frac{2n+1}{2h}\pi y\right)\exp\left[-\alpha_n(z+w/2)\right] \tag{8}$$

where

$$\alpha_n=\sqrt{\left(\frac{2n+1}{2h}\pi\right)^2-k^2}\ .$$

[1]We only consider the antisymmetric case of H_x since, if the incident field which includes the TEM wave is symmetric, there is no induced current on the resistive sheet. We can easily write down the traveling waves in regions II and III: $H_{x\mathrm{II}}(y,z)=H_{x\mathrm{III}}(y,z)=H_{xi}(y,z)$. These satisfy (2b), (3b), (5), and (7). This means that the resistive sheet does not influence the TEM wave at all.

The reflected field can be expressed in terms of an infinite series as follows:

$$H_{xr}(y,z)=\sum_{n=0} a_n \sin\left(\frac{2n+1}{2h}\pi y\right)\exp\left[\alpha_n(z+w/2)\right] \tag{9}$$

where the a_n are unknown coefficients to be determined later.

Region II: In this region both transmitted and reflected waves exist, due to the sheet. Consider condition (5) and $E_z|_{y=\pm h}=0$. We can express H_x as

$$H_{x\mathrm{II}}(y,z)=\pm\sum_{n=0}\left(b_n\exp\left[-\beta_n(z+w/2)\right]+c_n\exp\left[\beta_n(z-w/2)\right]\right)\cos\gamma_n(h\mp y),\qquad y\gtrless 0 \tag{10}$$

where $\beta_n=\sqrt{\gamma_n^2-k^2}$, and the γ_n are undetermined eigenvalues.

Region III: There is only a transmitted wave in this region. It is

$$H_{x\mathrm{III}}(y,z)=\sum_{n=0} d_n \sin\left(\frac{2n+1}{2h}\pi y\right)\exp\left[-\alpha_n(z-w/2)\right]. \tag{11}$$

IV. Coefficient Equations

In the formal solutions (9)–(11) the unknown coefficients a_n, b_n, c_n, d_n, and the eigenvalues γ_n are to be determined from boundary conditions (2b), (3b), (5), (7). At $y=0$, $|z|\leqslant w/2$, (10) satisfies (5) automatically. Substituting (10) into (7), we get

$$\sum_{n=0}\left(b_n\exp\left[-\beta_n(z+w/2)\right]+c_n\exp\left[\beta_n(z-w/2)\right]\right)\cdot\left(2\cos(h\gamma_n)-\frac{j\gamma_n}{\omega\epsilon_0 R}\sin(h\gamma_n)\right)=0. \tag{12}$$

This equation can be satisfied if

$$(h\gamma_n)\tan(h\gamma_n)=jr_M \tag{13}$$

where $r_M=2khR/R_0$ and $R_0=\sqrt{\mu_0/\epsilon_0}=120\pi\Omega$. Substituting (8)–(10) into (2b), we get

$$\sum_{n=0}(g_n+a_n)\sin\left(\frac{2n+1}{2h}\pi y\right)=\pm\sum_{n=0}\left(b_n+c_n\exp(-\beta_n w)\right)\cos\gamma_n(h\mp y),\qquad y\gtrless 0. \tag{14}$$

Multiplying each side by $\sin((2m+1/2h)\pi y)dy$ and integrating from $-h$ to h, we obtain

$$g_m+a_m=\sum_{n=0} L_{m,n}\left(b_n+c_n e^{-\beta_n w}\right),\qquad m=0,1,2,\cdots \tag{15}$$

where

$$L_{m,n}=\frac{\int_0^h \sin\left(\frac{2m+1}{2h}\pi y\right)\cos\gamma_n(h-y)dy}{\int_0^h\left[\sin\left(\frac{2m+1}{2h}\pi y\right)\right]^2 dy}$$
$$=\frac{\pi(2m+1)\cos(\gamma_n h)}{\left[\left(\frac{2m+1}{2}\pi\right)^2-(\gamma_n h)^2\right]}. \quad (15a)$$

From

$$\frac{\partial H_{x\mathrm{I}}}{\partial z}=\frac{\partial H_{x\mathrm{II}}}{\partial z}$$

of (2b) we have

$$\sum_{n=0}(g_n-a_n)\alpha_n\sin\left(\frac{2n+1}{2h}\pi y\right)$$
$$=\pm\sum_{n=0}(b_n-c_n\exp(-\beta_n w))\beta_n\cos\gamma_n(h\mp y), \quad y\gtrless 0.$$

Using the same procedure as above, we get

$$(g_m-a_m)\alpha_m=\sum_{n=0}L_{m,n}(b_n-c_n\exp(-\beta_n w))\beta_n, \quad m=0,1,2,\cdots. \quad (16)$$

Also at $z=w/2$ from (3b) we have

$$d_m=\sum_{n=0}L_{m,n}(b_n\exp(-\beta_n w)+c_n), \quad m=0,1,2,\cdots \quad (17)$$

$$d_m\alpha_m=\sum_{n=0}L_{m,n}(b_n\exp(-\beta_n w)-c_n)\beta_n, \quad m=0,1,2,\cdots. \quad (18)$$

V. Solution

We have derived (13) to determine the eigenvalues γ_n or propagation constants β_n, and four sets of equations (15)–(18) to determine the four sets of coefficients a_n, b_n, c_n, d_n. These sets of equations can be reduced. From (15) and (16) eliminating a_n we get

$$\sum_{n=0}L_{m,n}\left[b_n\left(1+\frac{\beta_n}{\alpha_m}\right)+c_n\left(1-\frac{\beta_n}{\alpha_m}\right)\exp(-\beta_n w)\right]=2g_m, \quad m=0,1,2,\cdots. \quad (19)$$

From (17) and (18) eliminating d_n we get

$$\sum_{n=0}L_{m,n}\left[b_n\left(1-\frac{\beta_n}{\alpha_m}\right)e^{-\beta_n w}+c_n\left(1+\frac{\beta_n}{\alpha_m}\right)\right]=0, \quad m=0,1,2,\cdots. \quad (20)$$

Let us now form (19)$\pm$(20). We finally get two independent sets of equations:

$$\sum_{n=0}S^{\pm}_{m,n}f^{\pm}_n=g_m, \quad m=0,1,2,\cdots \quad (21)$$

where

TABLE I
Real and Imaginary Parts of $\gamma_n h$ for Different r_M

n	r_M = 0.1	r_M = 2	r_M = 10
0	0.2273 + j0.2198	1.1739 + j0.5808	1.5547 + j0.1567
1	3.1418 + j0.0318	3.3106 + j0.6486	4.6486 + j0.5016
2	6.2832 + j0.0159	6.3015 + j0.3277	7.8382 + j0.9662
3	9.4248 + j0.0106	9.4298 + j0.2152	10.1290 + j1.3499
4	12.5664 + j0.0080	12.5685 + j0.1605	12.7242 + j1.0279
5	15.7080 + j0.0064	15.7090 + j0.1280	15.7578 + j0.7451
6	18.8500 + j0.0053	18.8502 + j0.1065	18.8727 + j0.5890
7	21.9911 + j0.0046	21.9915 + j0.0912	22.0039 + j0.4900

TABLE II
Real and Imaginary Parts of $L_{m,n}$ for $r_M=10$

m	n = 0	n = 1
0	1.0067 - j0.0496	-0.0089 - j0.0846
1	0.0096 - j0.0746	-1.0464 + j0.0451
2	0.0046 - j0.0416	-0.0509 + j0.1974
3	0.0031 - j0.0292	-0.0213 + j0.1143
m	n = 2	n = 3
0	-0.0019 + j0.0633	0.0369 - j0.0475
1	0.0298 + j0.2817	0.1244 - j0.1831
2	1.1693 + j0.0059	0.2033 - j0.6103
3	0.1912 - j0.3347	-1.2094 - j0.3710

$$S^{\pm}_{m,n}=\frac{L_{m,n}(1+\beta_n/\alpha_m\pm(1-\beta_n/\alpha_m)\exp(-\beta_n w))}{2},$$

$$f^{\pm}_n=(b_n\pm c_n).$$

In order to solve (21), we must solve (13) for γ_n and evaluate $S^{\pm}_{m,n}$. After using the iterated interpolation method to solve (13), we get the real and imaginary parts of $\gamma_n h$ for different r_M (Table I). Real and imaginary parts of $L_{m,n}$ for $r_M=10$ are give in Table II. We can see that the $L_{m,n}$ are very small except $L_{m,m}$. This is true in the range $r_M>5$.[2] In this case, we can neglect the terms $n\neq m$ and get the solutions of the coefficients a_n and d_n

$$a_n=\frac{g_n(1-\beta_n^2/\alpha_n^2)(1-\exp(-2w\beta_n))}{\left[(1+\beta_n/\alpha_n)^2-(1-\beta_n/\alpha_n)^2\exp(-2w\beta_n)\right]} \quad (22)$$

$$d_n=\frac{4g_n(\beta_n/\alpha_n)\exp(-w\beta_n)}{\left[(1+\beta_n/\alpha_n)^2-(1-\beta_n/\alpha_n)^2\exp(-2w\beta_n)\right]}. \quad (23)$$

Let the height h be chosen such that only the lowest TM mode can propagate, i.e., $\lambda/4<h<3\lambda/4$. Then the incident field (8) becomes $g_n=0$ except for g_0, and all of the coefficients are zero except for $n=0$. Finally, we get the reflection and transmission coefficients of the TM_{01}

[2] From (13) we see that when $n\pi\gg r_M$, $\gamma_n h\approx n\pi$ (see Table I). This suggests that the $L_{m,n}$ have a very good convergent behavior. From the definition of $L_{m,n}$ in (15a), when $n>m$, $\cos\gamma_n h=(-1)^n$ and $L_{m,n}$ decreases inversely as the square of n ($L_{m,n}\approx 1/n^2$).

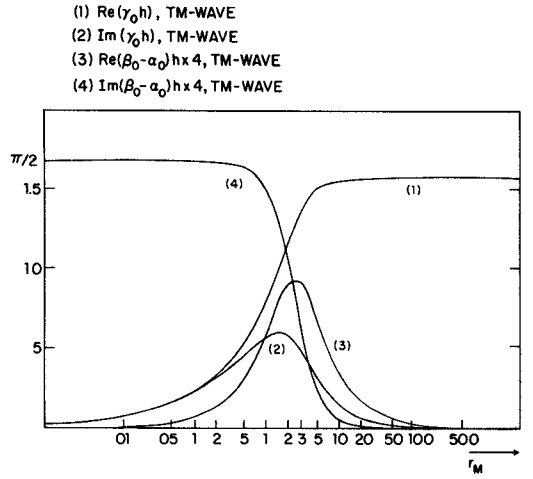

Fig. 2. Real and imaginary parts of $\gamma_0 h$ and $(\beta_0-\alpha_0)h$ as functions of r_M; $kh=\pi$.

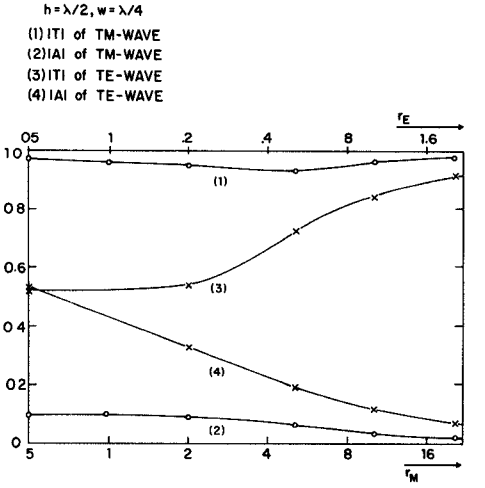

Fig. 3. $|T|$ and $|A|$ as functions of r_M and r_E.

were caused by the resistive sheet. They are [3]

$$A=-a_0/g_0$$

$$=-\frac{(1-\beta_0^2/\alpha_0^2)(1-\exp(-2w\beta_0))}{\left[(1+\beta_0/\alpha_0)^2-(1-\beta_0/\alpha_0)^2\exp(-2w\beta_0)\right]} \tag{24}$$

$$T=d_0/g_0$$

$$=\frac{4(\beta_0/\alpha_0)\exp(-w\beta_0)}{\left[(1+\beta_0/\alpha_0)^2-(1-\beta_0/\alpha_0)^2\exp(-2w\beta_0)\right]}. \tag{25}$$

The quantities $\gamma_0 h$, $\beta_0 h$ are plotted in Fig. 2 as functions of r_M.

In order to see the physical significance of formulas (24) and (25), we reduce them further. Because $\beta_0 \approx \alpha_0$ and Re $\beta_0 > 0$, the second term in the denominator is much smaller than the first term. After neglecting it, we get

$$A \doteq [(\beta_0-\alpha_0)/(\beta_0+\alpha_0)] + [(\alpha_0-\beta_0)/(\alpha_0+\beta_0)]\exp(-2w\beta_R)\exp(-j2w\beta_I) \tag{24a}$$

$$T \doteq \exp(-w\beta_R)\exp(-jw\beta_I) \tag{25a}$$

where $\beta_0=\beta_R+j\beta_I$. In (24a), the first term is the wave reflected from $z=-w/2$, and the second term is the wave reflected from $z=w/2$ which has a larger amplitude decay ($\exp(-2w\beta_R)$) and phase delay ($\exp(-j2w\beta_I)$). The factor 2 before w is due to the fact that the second reflected wave passes the resistive sheet twice. In (25a), the amplitude decay and phase delay of the transmitted wave are without the factor 2, because the wave passes the resistive sheet only once. The $|A|$ and $|T|$ values are plotted in Figs. 3 and 4 as functions of r_M and w/λ, respectively.

VI. The Resistive Sheet as Absorber

The resistive sheet can be used as an absorber. As shown in Fig. 5, the parallel-plate waveguide is terminated

[3]The definition of A is $A=E_{yr}/E_{yi}=-a_0/g_0$.

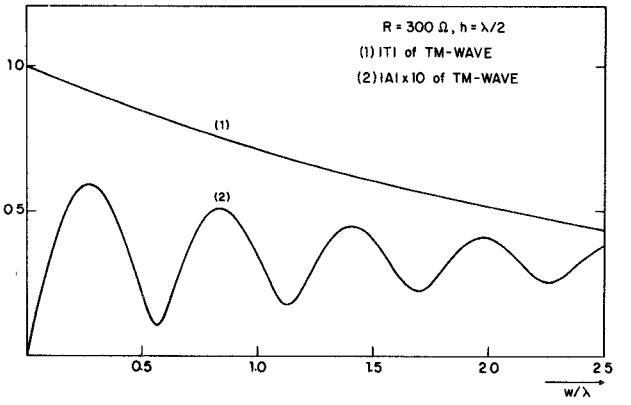

Fig. 4. $|T|$ and $|A|$ as functions of w/λ.

by a short-circuiting piston. We want to choose the resistance R, sheet width w, and position p such that the reflected wave is minimal. In this case, the general solutions are the same, but in region III:

$$H_{x\mathrm{III}}(y,z)=\sum_{n=0} d_n \sin\left(\frac{2n+1}{2h}\pi y\right)\cosh\alpha_n(z-p-w/2). \tag{26}$$

Using the same procedure, we get the equations for the coefficients:

$$g_m+a_m=\sum_{n=0} L_{m,n}(b_n+c_n\exp(-w\beta_n))$$

$$g_m-a_m=\sum_{n=0} L_{m,n}(b_n-c_n\exp(-w\beta_n))\beta_n/\alpha_m$$

$$d_m\cosh\alpha_m p=\sum_{n=0} L_{m,n}(b_n\exp(-w\beta_n)+c_n)$$

$$-d_m\sinh\alpha_m p=\sum_{n=0} L_{m,n}(b_n\exp(-w\beta_n)-c_n)\beta_n/\alpha_m. \tag{27}$$

The reflection coefficient of the TM_{01} wave is

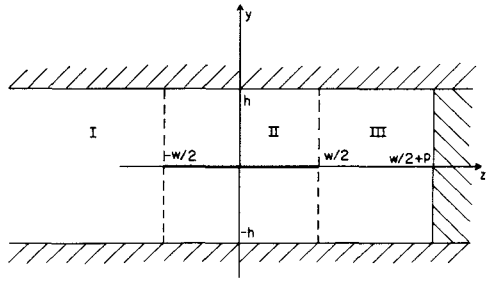

Fig. 5. The resistive absorber.

$$A=\frac{\beta_0-\alpha_0}{\beta_0+\alpha_0}$$

$$-\frac{\dfrac{\beta_0/\alpha_0-j\tan\alpha_I p}{\beta_0/\alpha_0+j\tan\alpha_I p}\exp(-2w\beta_0)}{\left[1-\dfrac{(\beta_0-\alpha_0)(\beta_0/\alpha_0-j\tan\alpha_I p)}{(\beta_0+\alpha_0)(\beta_0/\alpha_0+j\tan\alpha_I p)}\exp(-2w\beta_0)\right]}$$

$$\doteq(\beta_0-\alpha_0)/(\beta_0+\alpha_0)$$
$$-\exp(-2w\beta_R)\exp(-j2(w\beta_I+\alpha_I p)). \quad (28)$$

The physical significance of (28) is evident. The first term represents the wave reflected by the sheet, and the second term represents the wave reflected by the metal piston, where $\exp(-2w\beta_R)$ is the decay factor and $\exp(-j2(w\beta_I+\alpha_I p))$ is the phase delay. The appearance of the factor 2 is due to the fact that the wave passes the sheet twice; the minus sign is due to the phase reversal at the metal piston.

The maximum absorption occurs when A is equal to zero. From (28) we have

$$w=\left\{\ln\left[(\beta_I+\alpha_I)^2+\beta_R^2\right]-\ln\left[(\beta_I-\alpha_I)^2+\beta_R^2\right]\right\}/4\beta_R$$

$$p=\frac{\left[2\pi k-2w\beta_I+\tan^{-1}\left(\dfrac{\beta_I+\alpha_I}{\beta_R}\right)-\tan^{-1}\left(\dfrac{\beta_I-\alpha_I}{\beta_R}\right)\right]}{2\alpha_I}. \quad (29)$$

For example, if $r_M=2$, $h=\lambda/2$, it follows that $\lambda\alpha_I=5.4414$, $\lambda\beta_R=0.4576$, and $\lambda\beta_I=5.9602$. From (29) we obtain $w=3.0628\lambda$ and $p=0.1721\lambda$. Fig. 6 shows A as a function of p/λ for selected values of w.

VII. The TE Wave

From the boundary conditions (2a), (3a), (4), (6) for the TE wave, the general solutions are

$$E_{xi}(y,z)=\sum_{n=0} g_n\exp\left(-\alpha_n\left(z+\frac{w}{2}\right)\right)\cos\left(\frac{2n+1}{2h}\pi y\right) \quad (30)$$

$$E_{xr}(y,z)=\sum_{n=0} a_n\exp\left(+\alpha_n\left(z+\frac{w}{2}\right)\right)\cos\left(\frac{2n+1}{2h}\pi y\right) \quad (31)$$

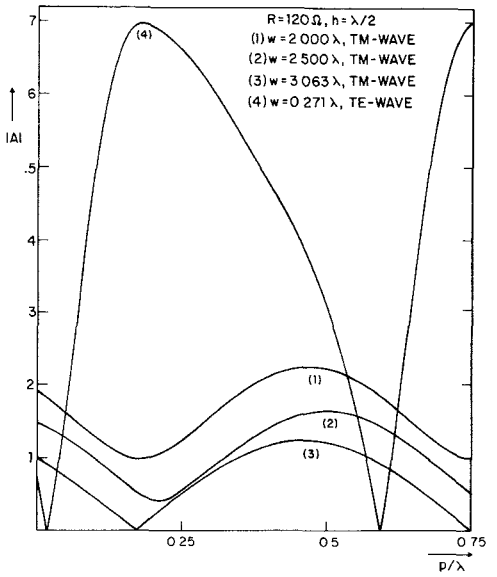

Fig. 6. $|A|$ as a function of p/λ.

TABLE III
Real and Imaginary Parts of $L_{m,n}$ for $r_E=1$

m	n = 0	n = 1	n = 2
0	1.1384 + j0.1128	-0.0107 - j0.1023	0.0012 + j0.0340
1	-0.0006 - j0.1167	-1.0093 - j0.0222	0.0026 + j0.0509
2	-0.0028 - j0.0384	-0.0025 + j0.0518	1.0029 + j0.0081
3	-0.0017 - j0.0191	-0.0004 + j0.0207	0.0011 - j0.0340
4	-0.0011 - j0.0115	-0.0001 + j0.0115	0.0002 - j0.0145
5	-0.0008 - j0.0076	-0.0000 + j0.0074	0.0001 - j0.0085

m	n = 3	n = 4	n = 5
0	-0.0003 - j0.0170	0.0001 + j0.0102	-0.0000 - j0.0068
1	-0.0004 - j0.0203	0.0001 + j0.0113	-0.0000 - j0.0072
2	-0.0011 - j0.0339	0.0002 + j0.0145	-0.0001 - j0.0085
3	-1.0014 - j0.0041	0.0006 + j0.0254	-0.0002 - j0.0113
4	-0.0006 + j0.0254	1.0009 + j0.0025	-0.0004 - j0.0203
5	-0.0002 + j0.0113	0.0004 - j0.0203	-1.0006 - j0.0017

$$E_{x\mathrm{II}}(y,z)=\sum_{n=0}\left[b_n\exp\left(-\beta_n\left(z+\frac{w}{2}\right)\right)+c_n\exp\left(\beta_n\left(z-\frac{w}{2}\right)\right)\right]\sin\gamma_n(h\mp y), \quad y\gtrless 0 \quad (32)$$

$$E_{x\mathrm{III}}(y,z)=\sum_{n=0} d_n\exp\left(-\alpha_n\left(z-\frac{w}{2}\right)\right)\cos\left(\frac{2n+1}{2h}\pi y\right). \quad (33)$$

Substituting (32) into (6) we get

$$\cot\gamma_n h=j/r_E\gamma_n h, \qquad r_E=2R/khR_0. \quad (34)$$

Substituting (30)–(33) into (2a) and (3a), we obtain the equations for the coefficients

$$(g_m+a_m)=\sum_{n=0} L_{m,n}(b_n+c_n\exp(-w\beta_n)),$$
$$m=0,1,2,\cdots \quad (35)$$

$$\alpha_m(g_m - a_m) = \sum_{n=0} L_{m,n}(b_n - c_n \exp(-w\beta_n))\beta n, \quad m=0, 1, 2, \cdots \quad (36)$$

$$d_m = \sum_{n=0} L_{m,n}(b_n \exp(-w\beta_n) + c_n), \quad m=0, 1, 2, \cdots \quad (37)$$

$$\alpha_m d_m = \sum_{n=0} L_{m,n}(b_n \exp(-w\beta_n) - c_n)\beta_n, \quad m=0, 1, 2, \cdots \quad (38)$$

where

$$L_{m,n} = \frac{\int_0^h \sin \gamma_n(h-y)\cos\left(\frac{2m+1}{2h}\pi y\right)dy}{\int_0^h \left[\cos\left(\frac{2m+1}{2h}\pi y\right)\right]^2 dy} = \frac{2\gamma_n h \cos \gamma_n h}{\left[\left(\frac{2m+1}{2}\pi\right)^2 - (\gamma_n h)^2\right]}. \quad (39)$$

The form of (35)–(38) is exactly the same as (15)–(18) except the values of β_n and $L_{m,n}$ are different because the eigenequation (34) and the definition of $L_{m,n}$ in (39) are different. Thus, we have the same formal solutions (22) and (23) and, for the absorber, the solution is the same as (28).

The quantities $\gamma_0 h$, $\beta_0 h$ are plotted in Fig. 7 as functions of r_E. In Fig. 8 $|A|$ and $|T|$ are shown as functions of w/λ; they are plotted as functions of r_E in Fig. 3. The $L_{m,n}$ are listed in Table III for $r_E = 1$.

VIII. Conclusion

All effects due to the presence of a resistive sheet have been determined by the parameter r_M or r_E for the TM or TE wave, respectively. The sensitive ranges of r are 0.2–20 for the TM wave, 0.02–2 for the TE wave (see Figs. 2, 3, and 7).

Both the TM wave and the TE wave have the maximum decay coefficient $\beta_R(r)$ (see Figs. 2 and 7): for the TM wave at $r_M = 2$, for the TE wave at $r_E = 0.2$. From these two conditions, we can determine the resistance R and height h such that both the TM wave and the TE wave are subjected to maximum absorption. Because $r_M \cdot r_E = (2R/R_0)^2$, we obtain $R = 120\ \Omega$ and $h = \lambda/2$.

The decay coefficient of the TE wave is much larger than that of the TM wave. Because the sheet extends to infinity in the x-direction, it interacts effectively with the TE wave which has an E_x component. Fig. 9 shows that β_R of the TE wave is 5 times that of the TM wave.

With the sheet as an absorber both TM and TE waves have points of maximum absorption, but the absorption of the TE wave is more evident as shown in Fig. 6. The optimum width for the TE wave is much more shorter than that for the TM wave. When $R = 120\ \Omega$, $w \doteq \lambda/4$ for the TE wave and $w \doteq 3\lambda$ for the TM wave.

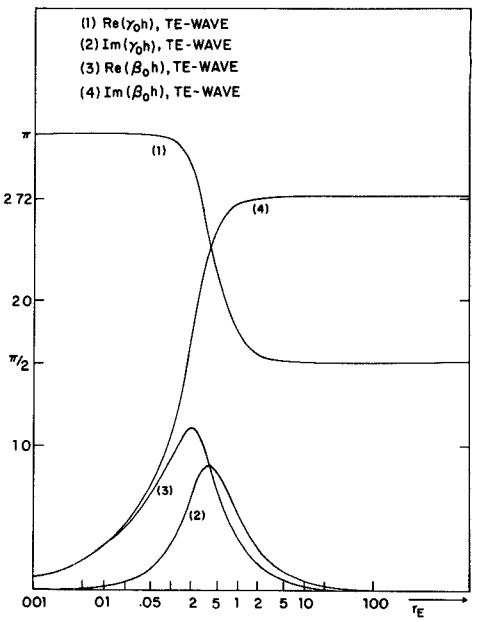

Fig. 7. Real and imaginary parts of $\gamma_0 h$ and $\beta_0 h$ as functions of r_E; $kh = \pi$.

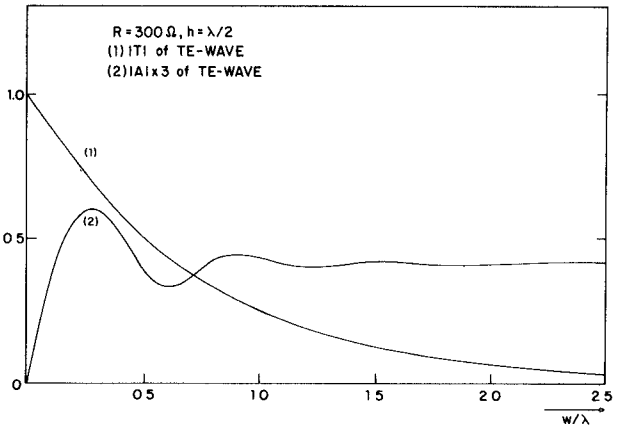

Fig. 8. $|T|$ and $|A|$ as functions of w/λ.

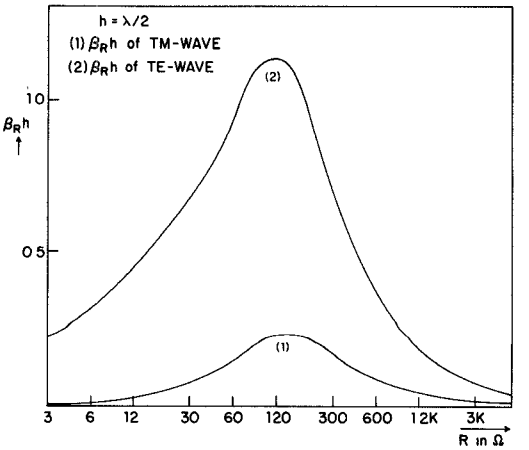

Fig. 9. Comparison of decay coefficients.

TABLE IV
TRANSMISSION COEFFICIENTS T AND REFLECTION COEFFICIENTS A OBTAINED USING N TERMS IN SIMULTANEOUS EQUATIONS (21)

N	$r_M = 0.1$	$r_M = 2$	$r_M = 10$
		T of TM Wave	
1	$0.9820e^{-j1.5698}$	$0.8904e^{-j1.4838}$	$0.9569e^{-j1.3677}$
2	$0.9815e^{-j1.5413}$	$0.9149e^{-j1.4680}$	$0.9576e^{-j1.3700}$
4	$0.9887e^{-j1.4976}$	$0.9395e^{-j1.4560}$	$0.9596e^{-j1.3735}$
6	$0.9905e^{-j1.4843}$	$0.9465e^{-j1.4503}$	$0.9626e^{-j1.3754}$
8	$0.9908e^{-j1.4780}$	$0.9507e^{-j1.4460}$	$0.9626e^{-j1.3758}$
		A of TM Wave	
1	$0.1417e^{-j0.0345}$	$0.1084e^{-j0.6093}$	$0.0310e^{-j1.1921}$
2	$0.1506e^{-j0.0138}$	$0.1074e^{-j0.6307}$	$0.0310e^{-j1.1884}$
4	$0.1188e^{+j0.0397}$	$0.0945e^{-j0.4864}$	$0.0301e^{-j1.1995}$
6	$0.1087e^{+j0.0553}$	$0.0891e^{-j0.4417}$	$0.0325e^{-j1.1400}$
8	$0.1042e^{+j0.0615}$	$0.0853e^{-j0.4143}$	$0.0320e^{-j1.1000}$

The solutions (22)–(25) and (28) are of first-order, but they have sufficient accuracy over a wide range of resistances R. Table IV shows a comparison between the solutions that have been obtained using different numbers N of terms in the simultaneous equations (21). Because the incident field has only one term ($g_n = \delta_{n0}$) and $S^{\pm}_{m,n}$ converges more rapidly, the solutions change little when the number N of terms is larger than 4. When $r_M > 2$, the relative error in the first-order solution is less than 3 percent. Thus the formulas (22)–(25), (28), and (29) can be used in practical cases with sufficient accuracy.

ACKNOWLEDGMENT

This work was performed under the guidance of Prof. R. W. P. King and Prof. T. T. Wu. The author is grateful to them for their advice and help. He also wishes to thank Dr. Carl E. Baum and Dr. David V. Giri for proposing this problem, and Ms. Margaret Owens and Ms. Jill Friedlander for their help in correcting and typing the manuscript.

REFERENCES

[1] P. Moon and D. E. Spencer, *Field Theory Handbook*. Berlin, Germany: Springer-Verlag, 1971.
[2] S. A. Schelkunoff, "Theory of antennas of arbitrary size and shape," *Proc. IRE*, vol. 29, p. 493, 1941.
[3] C. C. Rogers, J. K. Schindler, and F. Y. Schultz, "The scattering of a plane electromagnetic wave by a finite cone," in *Electromagnetic Theory and Antennas*, E. C. Jordan, Ed. New York: The Macmillan Co., 1963, pp. 67–80.
[4] A. Wexler, "Solution of waveguide discontinuities by modal analysis," *IEEE Trans. Microwave Theory Tech.*, vol. MTT-15, pp. 508–517, Sept. 1967.
[5] H.-M. Shen, "On the theory of scattering by a spherical mirror," *Acta Phys. Sin.*, vol. 27, pp. 533–546, Sept. 1978.